Transactions on Modelling and Simulation vol 11, © 1995 WIT Press, www.witpress.com, ISSN 1743-355X

Numerical and experimental analysis of liquid sloshing in rectangular containers

V. Armenio[a], M. La Rocca[b]

[a]*Department of Naval Architecture, Ocean and Environmental Engineering, University of Trieste, via Valerio 10, 34127, Trieste, Italy*

[b]*Department of Science of Civil Engineering, III University of Rome, via C. Segre, 00145 Rome, Italy*

Abstract

In this paper sloshing of water in rectangular containers is extensively analysed. Two different mathematical models are employed, the Reynolds Averaged Navier-Stokes equations and the Shallow Water equations. RANSe are solved by means of a semi-implicit formulation of the well established MAC method, SWe are solved by using an algorithm developed in the framework of gas dynamics for hyperbolic equations. In order to validate the mathematical models, experimental tests have been carried out using a 0.5m breadth open tank in periodic roll motion. Numerical results by RANSe compare fairly well in the whole range of cases investigated, in particular both hydraulic jumps and travelling waves are well simulated On the other hand, this study has shown that the shallow water equations can be efficiently used up to liquid depth to tank breadth ratio equal to 0.15.

1 Introduction

Sloshing of liquids in compartments typically exhibits non linear characteristics. Depending on the tank geometry, on the external excitation and on the liquid viscosity several wave modes appear, standing waves, travelling waves or hydraulic jumps when the liquid depth inside the tank is small enough. Often the superposition of the above wave modes results into large dynamic loads over the walls of the flooded tank, generating a large heeling moment or the rising of large impulsive pressure peaks.

In maritime applications the problem is twofold: from a structural viewpoint particular attention must be devoted to tank failures in LNG tankers because of the risk of brittle fractures of the primary structure, and of the consequent expensive repair costs. On the other hand the analysis of the dynamic response of ships with flooded compartments is becoming more and more important in the study of ship stability as far as capsizing is concerned [1].

The theoretical evaluation of sloshing induced loads is generally a difficult task. The linear theory provides the resonance frequencies of the system when the tank geometry is sufficiently simplified [2]. An appropriate approach to the problem involves the solution of the Navier-Stokes equations including the non linear boundary conditions over the free surface. Recently a MAC-type method [3] has been used for the evaluation of the sloshing induced loads in rectangular or prismatic baffled tanks. Unfortunately due to the characteristics of the above algorithm, only a rough investigation of viscous effects upon the sloshing induced loads has been carried out.

On the other hand, when the liquid depth to tank breadth ratio (λ/B) is small enough the shallow water approximation yields a fairly good estimation of the wave profile even in the case of large amplitude excitation. In the past Dillingham [4] has used the above equations to investigate the dynamic effects of water shipped on deck of a small fishing vessel on its own transversal stability.

The SWe represent a strong approximation to the more complete Navier-Stokes equations, thus it appears an interesting task to investigate the accuracy of these mathematical models by means of comparisons with experimental results.

In this paper both RANS equations and SWe are solved numerically. RANSe are solved by using a modified form of MAC method, called SIMAC [5] (Semi-Implicit Marker and Cell Method), able to catch accurately either the free surface evolution and the boundary layer at the rigid walls. SW equations are solved by using a recent method (CE-SE) developed in the framework of gas dynamics by Chang and To [6].

Finally, experimental tests have been carried out at the Laboratories of the Dept. of Hydraulics of the University of Rome. Comparison are presented between numerical results and experimental data.

2 Mathematical models

As discussed above two different mathematical models are employed. In all cases two-dimensional computations have been carried out. The extension of the algorithms to three-dimensional computations is in progress. In the following a brief description of the algorithms used in this work for the solution of the above equations is given.

Solution of RANSe

In a frame of reference fixed to the body (Fig. 1) the Reynolds Averaged Navier Stokes equation are:

$$\frac{\partial u_i}{\partial x_i} = 0 \quad , \quad \frac{\partial u_i}{\partial t} + u_j \frac{\partial u_i}{\partial x_j} = - \frac{\partial P}{\partial x_i} + \frac{\partial}{\partial x_j} \left[-\overline{u_i' u_j'} + \nu \frac{\partial u_i}{\partial x_j} \right] + B_i \tag{1}$$

where the Reynolds stress is modelled by an eddy viscosity model:

$$- \overline{u_i' u_j'} = \nu_t \left[\frac{\partial u_i}{\partial x_j} + \frac{\partial u_j}{\partial x_i} \right] - \frac{2}{3} k \, \delta_{ij} \tag{2}$$

The eddy viscosity is calculated by a subgrid scale model as modified by Miyata [7] into a two-dimensional form.

On the free surface the dynamic condition $P = \frac{p - p_{atm}}{\rho} = 0$ and the non linear kinematic condition:

$$\frac{\partial \lambda}{\partial t} + u_1 \frac{\partial \lambda}{\partial x} - u_2 = 0 \tag{3}$$

are considered respectively. In eqn (3) $\lambda = \lambda(x,t)$ stands for the position of the free surface. In this work a modified form (SIMAC) of the well known MAC method is employed. SIMAC solves the RANS equations using a semi-implicit formulation of the momentum equation as described in [8]. The diffusive terms are treated implicitly by means of the 2nd order Crank-Nicholson scheme using the approximate factorisation technique, whereas the convective terms are discretized explicitly by means of the Adams-Bashforth scheme in time and of a second order upwinding scheme (HLPA) in space. The pressure equation is solved by means of a multigrid technique based on the Additive Correction strategy of Hutchinson and Raithby [9]. The previous acceleration technique applied to a free surface computation cuts down the CPU time by a factor 10 compared to a classical SOR procedure. Finally the free surface is treated as in TUMMAC V [10].

The main advantage of SIMAC on the previous MAC methods is in its own ability in dealing with very stretched grids at the rigid walls, making available realistic computations at very large Reynolds numbers. For a more detailed description of the method herein adopted refer to [5, 11].

Solution of SWe

It is known that when the liquid depth is small enough the Euler equations in the hypothesis of an inviscid liquid can be simplified in a more suitable hyperbolic form. Referring to the body-fixed frame of reference of Fig. 1 and considering the tank subjected to periodic roll motion, the shallow water approximation gives:

$$\frac{\partial \lambda}{\partial t} + \frac{\partial (\lambda u)}{\partial x} = 0 \tag{4}$$

$$\frac{\partial (\lambda u)}{\partial t} + \frac{\partial}{\partial x}\left[\lambda u^2 + g \cos\phi \frac{\lambda^2}{2} \right] = \lambda \left[- \dot{\Omega} \frac{\partial (\lambda x)}{\partial x} + \Omega^2 \lambda \frac{\partial \lambda}{\partial x} - 2 \Omega \frac{\partial (\lambda u)}{\partial x} + B_x \right] \tag{5}$$

In eqns (4) and (5) u represents the x-component of velocity averaged over the y-direction, ϕ, Ω and $\dot{\Omega}$ the roll angle, velocity and acceleration respectively, and B_x the x-component of the body forces acting throughout the liquid. The previous equations are hyperbolic in nature, and formally similar to the equations governing the motion of a gas into a mono-dimensional duct. Thus a numerical technique developed in the framework of gas dynamics can be successfully applied to our physical problem. In particular the CE-SE algorithm developed by Chang and To [6] is used in this work. In the above algorithm the space-time domain of integration of the governing equations is discretized into

two set of elements, solution elements(SEs) and conservation elements (CEs) respectively.

The above method is effective in simulating sharp discontinuities (hydraulic jumps) without appreciable loss of mass during the computation. The application of the CE-SE algorithm to free surface problems is presented with more details in [12].

3 Experimental setup

The experimental device used for validation of numerical results is evidenced in Fig. 2. It consists of a 0.5 m x 0.5 m x 0.25 m tank constructed with Plexiglas, posed upon a massive support anchored to the floor. An a.c. motor is used to get the tank in roll motion by means of a four-bar linkage. The maximum available frequency from the motor is f=1.08 s^{-1}. The free surface profile has been recorded by a digital video camera put 1.5 m far from the tank. Moreover a wave height recorder composed by an ultrasonic sensor (Honeywell S942-AUDS) has been put 0.10 m far from the right side wall of the tank.

4 Numerical and experimental results

Several tests have been carried out either numerically and experimentally. In particular four different liquid depths within the shallow water hypothesis have been considered, λ = 0.025 m, 0.05 m, 0.075 m and 0.10 m corresponding to λ/B = 0.05, 0.10, 0.15 and 0.20 respectively.

Firstly, decay tests have been performed numerically, considering as initial condition a flat free surface profile inclined by an angle of 5°. The computed non-dimensional natural periods compared to that derived by the linear theory are in Fig. 3. It appears that both the mathematical models provide a good estimation of the wave speed up to λ/B=0.15, whereas a further increasing of the liquid depth inside the tank causes the SWe to predict a smaller wave speed compared to analytical and RANSe results.

The analysis of forced response has been carried out in a wide range of roll frequencies including the resonant one, and considering two different amplitudes of roll motion, Φ_0 = 0.9° and 1.7°. The choice of small roll amplitudes was made in order to avoid outflow from the open tank in resonant motion.

For λ/B=0.05 numerical non-dimensional wave heights $\left[\frac{\lambda_{max} - \lambda_{min}}{B}\right]$ compare very well with experimental data (Fig. 4,5). A very interesting non linear phenomenon has been evidenced either numerically and in the experimental tests. The response curve shows the presence of a jump in the frequency domain. In particular for Φ_0=0.9° at ω = 3.98 rad/s two wave modes can be independently excited, a standing wave and a hydraulic jump respectively. For ϕ_0=1.7° the same phenomenon appears at ω=4.25 rad/s. Our computations and experiments confirm a previous theoretical work, in which water sloshing inside a compartment is modelled by a simplified hardening type spring-mass non linear system [13].

Comparison between computed and observed wave profiles are presented in Fig. 6,7.

Numerical and experimental results compare very well for $\lambda/B=0.10$ and $\lambda/B = 0.15$ also (Fig. 8,9). Nevertheless a large qualitative and quantitative disagreement between numerical results (SWe) and experimental data is obtained in the case $\lambda/B=0.20$ near resonance (Fig. 10). This is basically due to the fact that SWe always provide a jump-like wave in resonance, irrespective of the liquid depth inside the tank. The case $\lambda/B=0.20$, that in literature is considered as the limiting case for the application of the shallow water approximation, is characterised by the presence of large travelling waves rather than by hydraulic jumps. However solutions by RANSe provide accurate results in this case also.

5 Concluding Remarks

Sloshing of shallow water in rectangular containers has been investigated either numerically and by experiments.

Two different mathematical models have been employed, the RANSe and the SW equations respectively. A new efficient algorithm (SIMAC) able either to deal with very large impact waves and to solve accurately the viscous stresses has been used for solving RANSe, whereas a new and powerful method (CE-SE) has been applied to the solution of the shallow water equations.

Numerical results by RANSe compare fairly well with experimental data in the whole range of cases analysed.

It has been proved that the shallow water approximation is effective up to $\lambda/B=0.15$, whereas by increasing the liquid depth inside the tank the SWe predict results that present increasing discrepancies with experimental data.

The analysis is still in progress. At the moment the computer codes have been matched to a ship motion code, in order to analyse the effect of the coupling between the roll motion of a ship and liquid sloshing inside a flooded compartment.

References

1. Cleary, W. A. Jr Subdivision, stability, liability, *Marine Technology*, 1982. **19**, 228-244.

2. Abramson, H. N. The dynamic behaviour of liquids in moving containers, Report SP 106 of NASA, 1966.

3. Su, T. C., Lou, J. K., Flipse, J. E. & Bridges, T. J. A numerical analysis of large amplitude liquid sloshing in baffled containers, Report MA-RD-940-82046 of the Texas A&M University College Station, 1982.

4. Dillingham, J. T. Motion studies of a vessel with water on deck, *Marine Technology* , 1981, **18**, 38-50.

5. Armenio, V. A new algorithm (SIMAC) for the solution of free surface unsteady high Reynolds flows, pp. 3 to 6, *Proceedings of the 9th Int. Workshop on Water Waves and Floating Bodies,* Kuju, Oita, Japan, 1994.

6. Chang, S. C. & To, W. M. A brief description of a new numerical framework for solving conservation laws: the method of space-time conservation element

and solution element, pp. 396 to 400, *Proceedings of the . 13th Int. Conf. on Numerical Methods in Fluid Dynamics,* Rome, Italy, 1992.

7. Miyata, H., Kajitani, H., Zhu, M., Kavano, T. & Takai, M. Numerical study of some wave-breaking problems by a finite-difference method, *J. of Kansai Society of Naval Architects* ,1987, **207**, 11-23.

8. Huser, A. & Biringen, S. Calculation of two-dimensional shear-driven cavity at high Reynolds numbers, *Int. J. for Numerical Methods in Fluids* , 1992, **14**, 1087-1109.

9. Hutchinson, B. R. & Raithby, G. D. A multigrid method based on the additive correction strategy, *Num. Heat Transfer,* 1986, **9**, 511-537.

10. Miyata, H. Finite difference simulation of breaking waves, *J. of Computational Physics* , 1986, **65**, 179-214.

11. Armenio, V. 1994. SIMAC: a semi-implicit marker and cell method for unsteady free surface viscous flows, *paper submitted to Int. Journal of Num. Methods in Fluids*

12. La Rocca, M. On the roll motion of ships with free surface liquids on board: Solution of the hydrodynamic problem and experimental validation', *Ph.D Thesis, D.S.I.C. III University of Rome,* 1994.

13. Ockendon, J.R. and Ockendon, H. Resonant surface waves, *J. of Fluid Mechanics*, 1973, **59**, 397-413.

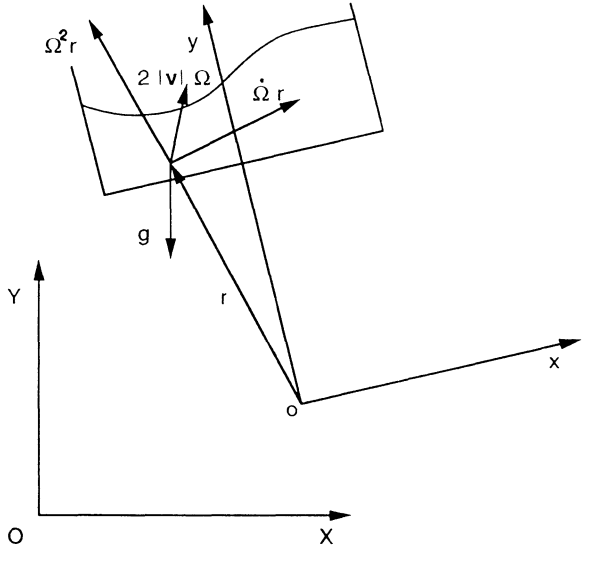

Figure 1: Frame of reference used in the mathematical models, and representation of the body forces per unitary volume acting on the liquid.

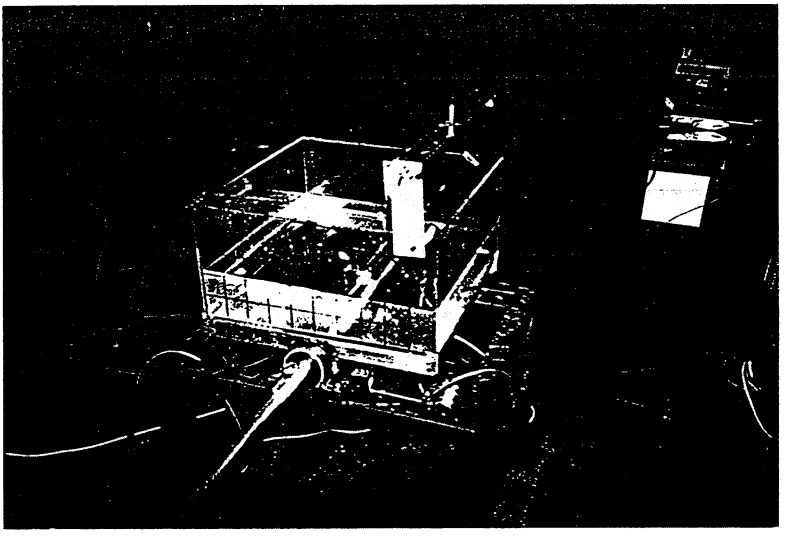

Figure 2: Perspective view of the experimental device

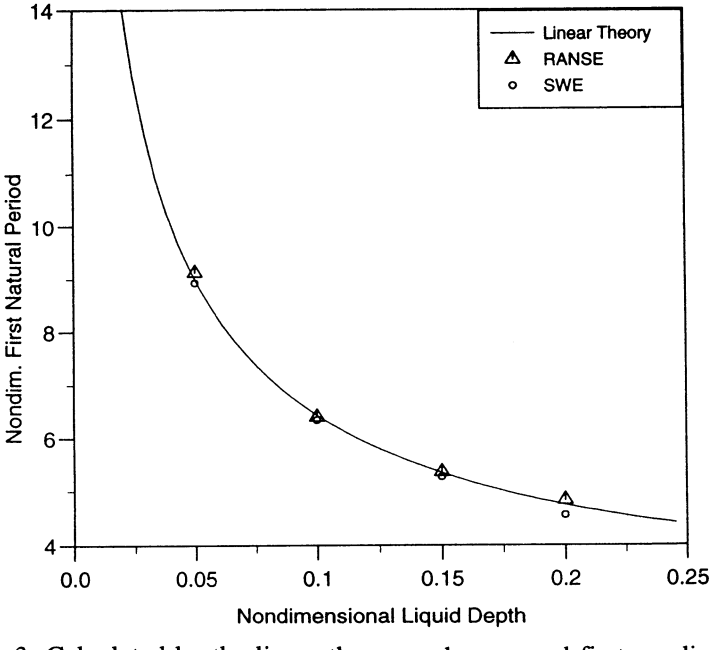

Figure 3: Calculated by the linear theory and computed first nondimensional natural period $\left[T\sqrt{\frac{g}{B}}\right]$ versus the nondimensional liquid depth.

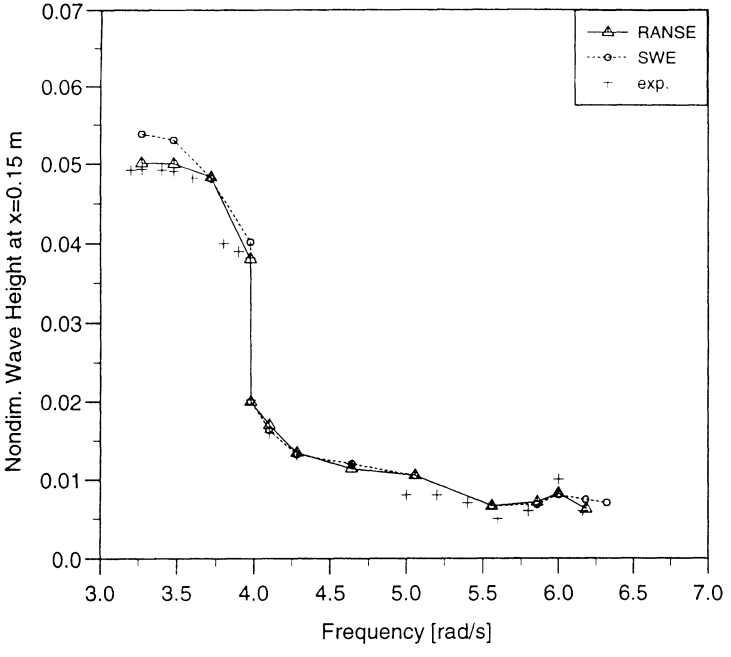

Figure 4:Computed and measured nondimensional wave heights versus roll frequency: $\lambda/B = 0.05$, maximum roll amplitude $\Phi_0 = 0.9°$.

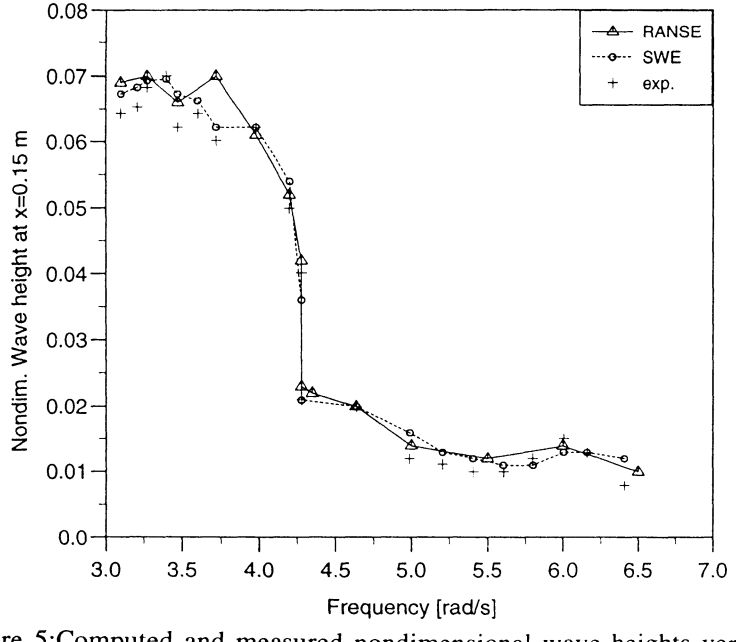

Figure 5:Computed and measured nondimensional wave heights versus roll frequency: $\lambda/B = 0.05$, maximum roll amplitude $\Phi_0 = 1.7°$.

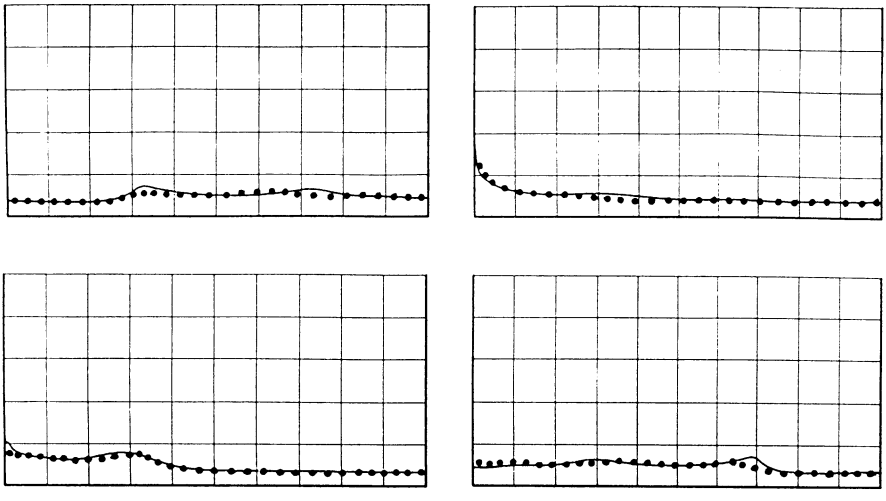

Figure 6:Computed by RANSe (—) and recorded (•) wave profiles in resonance conditions (ω = 3.47 rad/s, Φ_0 = 0.9°) for λ/B = 0.05, at four time instants: t_1 = 4.63 s, t_2 = 4.93 s, t_3 = 5.23 s, t_4 = 5.53 s.

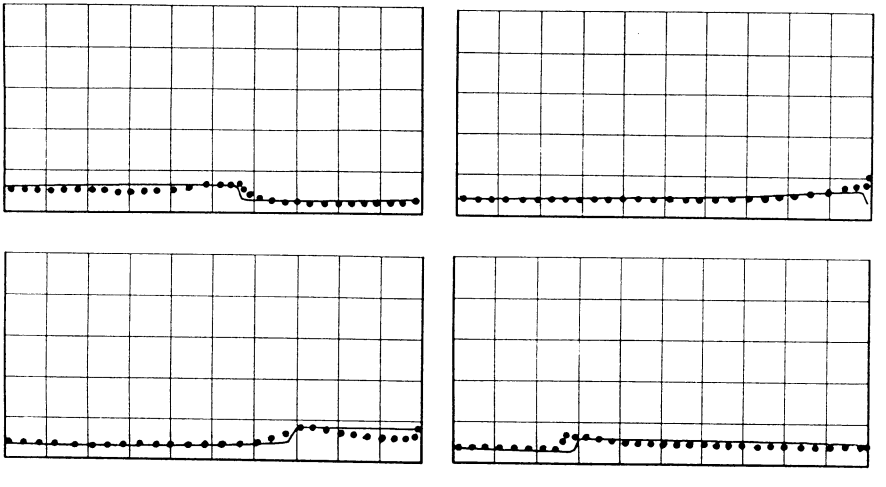

Figure 7: Computed by SWe (—) and recorded (•) wave profiles in resonance conditions (ω = 3.98 rad/s, Φ_0 = 1.7°) for λ/B = 0.05, at four time instants: t_1 = 5.15 s, t_2 = 5.45 s, t_3 = 5.75 s, t_4 = 6.05 s.

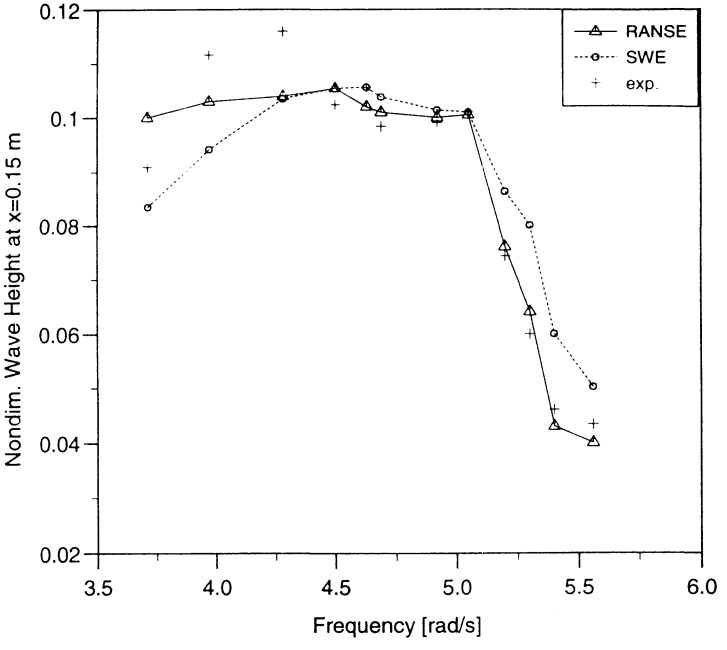

Figure 8: Computed and measured nondimensional wave height versus roll frequency: $\lambda/B = 0.10$, maximum roll amplitude $\Phi_0 = 1.7°$.

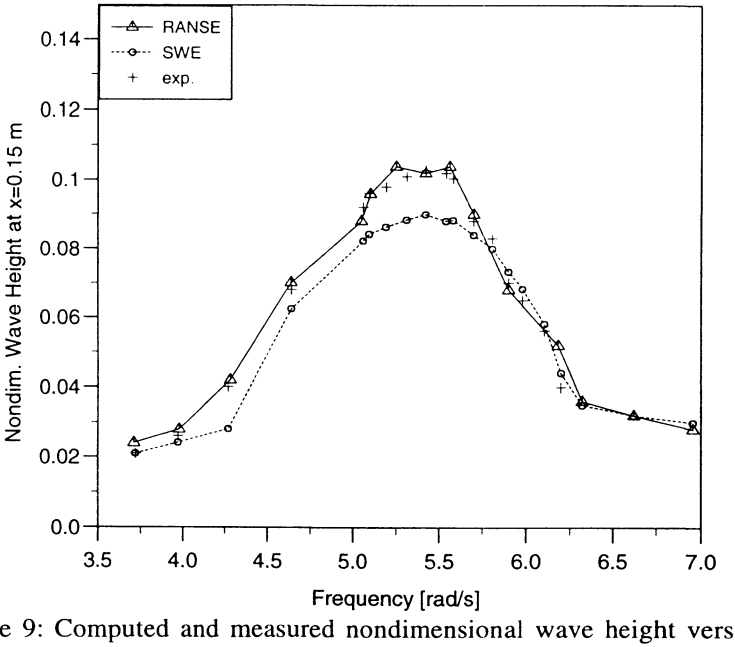

Figure 9: Computed and measured nondimensional wave height versus roll frequency: $\lambda/B = 0.15$, maximum roll amplitude $\Phi_0 = 0.9°$.

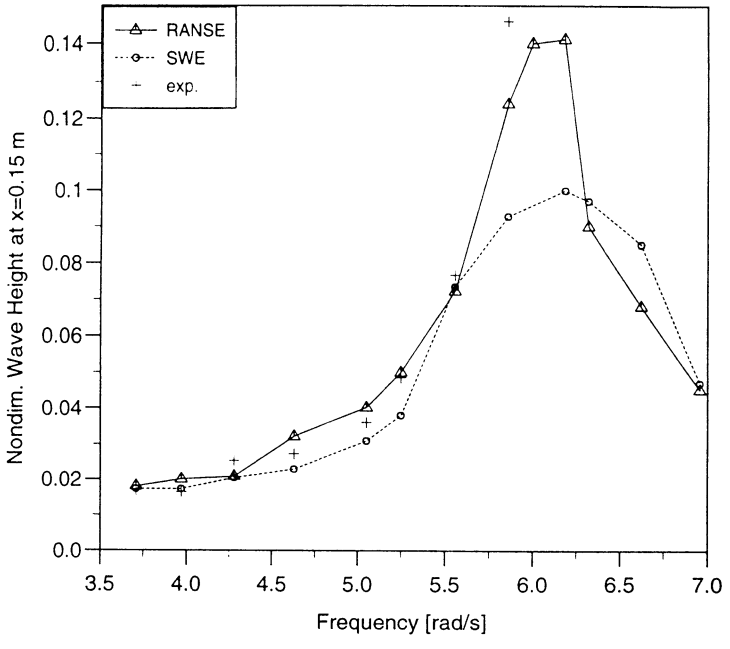

Fig. 10: Computed and measured nondimensional wave height versus roll frequencies: $\lambda/B = 0.20$, maximum roll amplitude $\Phi_0 = 0.9°$.